Article

Tree Diameter at Breast Height (DBH) Estimation Using an iPad Pro LiDAR Scanner: A Case Study in Boreal Forests, Ontario, Canada

Matthew Guenther *, Muditha K. Heenkenda, Dave Morris, Brigitte Leblon

Posted Date: 15 December 2023

doi: 10.20944/preprints202312.1133.v1

Keywords: iPad Pro LiDAR; DBH; Boreal Forest; Forest Inventory; Mobile Laser Scanning

Article

Tree Diameter at Breast Height (DBH) Estimation Using an iPad Pro LiDAR Scanner: A Case Study in Boreal Forests, Ontario, Canada

Matthew Guenther [1,*], Muditha K. Heenkenda [2], Dave Morris [3] and Brigitte Leblon [1]

[1] Faculty of Natural Resources Management, Lakehead University, 955 Oliver Road, Thunder Bay, ON, P7B 5E1; mguenthe@lakeheadu.ca, bleblon@lakeheadu.ca
[2] Department of Geography and the Environment, Lakehead University, 955 Oliver Road, Thunder Bay, ON, P7B 5E1; mheenken@lakeheadu.ca
[3] Centre for Northern Forest Ecosystem Research, Ontario Ministry of Natural Resources and Forestry, 421 James St S, Thunder Bay, ON, P7E 2V6; dave.m.morris@ontario.ca
* Correspondence: mguenthe@lakeheadu.ca

Abstract: This paper is a follow-up to a previous study that was conducted in a research forest and identified the optimal method for Diameter at Breast Height (DBH) estimation as a circular scanning and fitting ellipses to 4cm stem cross-sections at breast height. The aim of this study was to determine whether the identified method is applicable to natural boreal forests as well. The iPad Pro LiDAR scanner was used to acquire point clouds for 15 sites representing a range of natural boreal forest conditions in Ontario, Canada, and estimate DBH. The secondary objective was to determine if tested stand (Species composition, age, density, understory) or tree (Species, DBH) factors affected the accuracy of estimated DBH. Overall, estimated DBH values were within 1cm of actual DBH values for 78 of 133 measured trees (59%). An RMSE of 1.5cm (8.6%) was achieved. Stand age had a large effect (>0.15) on the accuracy of estimated DBH values, while density, understory, and DBH had moderate effects (0.05-0.14). No trend was identified between accuracy and stand age. Accuracy improved as understory density decreased and as tree DBH increased. Inertial Measurement Unit (IMU) and positional accuracy errors with the iPad Pro scanner limit the feasibility of using this device for forest inventories.

Keywords: iPad Pro LiDAR; DBH; boreal forest; forest inventory; mobile laser scanning

1. Introduction

Diameter at Breast Height (DBH) is the diameter of a tree stem 1.3m above the ground, and is a key variable measured in forest inventories [1,2]. DBH is traditionally measured manually using a diameter tape or callipers, but these methods are time-consuming and costly [3]. Light Detection and Ranging (LiDAR) is a remote sensing technology that has previously been used to accurately estimate DBH [2–5]. A key message from this previous work was the need to acquire data from multiple perspectives due to tree stems' irregular, uneven shapes [6,7]. High site densities and significant understory vegetation have also been found to contribute to error in estimated DBH values [8,9].

In 2020, Apple released the iPad Pro 12th Generation, a consumer tablet with an integrated LiDAR scanner with a scanning range up to 5m and an accuracy of ±1cm [5,10]. Previous studies have examined different acquisition and processing methods when using the iPad Pro LiDAR scanner to acquire point clouds for DBH estimation [2,5,11]. However, these studies have taken place in urban or plantation forests with minimal variation or obstruction within the scanned plots. Therefore, it is important to test the accuracy of DBH estimation with iPad Pro LiDAR in a range of natural boreal forest conditions. Therefore, this study aimed to explore the possibilities of using the iPad Pro LiDAR sensor within natural forests for DBH estimation.

This paper is a follow-up to our previous study where we compared multiple walking patterns for LiDAR point cloud acquisition with the iPad Pro, as well as multiple processing methods to

Preprints (www.preprints.org) | NOT PEER-REVIEWED | Posted: 15 December 2023 doi:10.20944/preprints202312.1133.v1

determine which combination of walking pattern and processing method produced the most accurate estimates of DBH [11]. Specific objectives of this study were to: (1) determine if site-level attributes (Age Class, Species Class, Tree Density, Understory Density) or tree-level attributes (Tree Species, DBH sizes) have statistically significant impacts on DBH estimate accuracy; and, (2) identify site conditions that facilitate or inhibit accurate estimates of DBH from LiDAR point cloud data. It is hypothesized that DBH estimate accuracy will be reduced in stands with significant leafy tissue at or around breast height, either sites with high understory densities or sites with high site densities (trees per ha). It is also hypothesized that DBH estimates will be more accurate for sites with larger tree sizes, as DBH estimate accuracy has been found to increase as measured DBH increases [11].

2. Materials and Methods

2.1. Study Area

LiDAR and model validation data was collected in 15 natural, wildfire-origin stands that represented five age classes (20-40 years, 41-60 years, 61-80 years, 81-100 years, and 101+ years) and three species groups (Broadleaf-dominated sites (BRD): 68-100% broadleaf, Coniferous sites (CON): 68-100% conifer, and mixed sites (MX): 33-67% conifer). The study sites were located in one of three Forest Management Units (FMUs) that adjoined each other: the Black Spruce, Dog River-Matawin, and English River FMUs. The sites sampled represented a selected sub-sample of the Ontario Ministry of Natural Resources and Forestry (OMNRF) Vegetation Sampling Network (VSN) plots. VSN plots were selected the previous year by the OMNRF using a Principal Component Analysis (PCA) using 26 structural attributes derived from recent aerial LiDAR (Single Photon) imagery to select sites representing the full range of structural variability present in a given FMU [12]. VSN plots are circular (400 m2), with a radius of 11.28m from a fixed plot center to the plot boundary. All VSN plot centers are marked on the ground with a metal rod to ensure each field crew visiting the site uses the same plot center. Below, Figure 1 shows the location of the sites selected for this study within northwestern Ontario, as well as their location within Ontario.

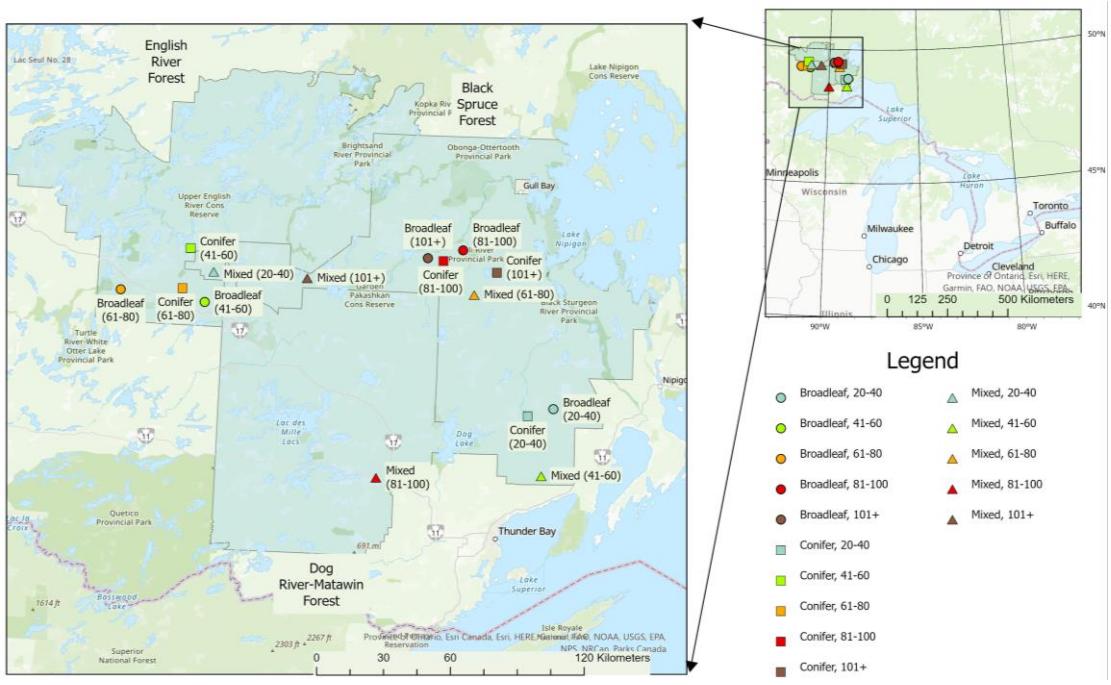

Figure 1. Map showing location of field sites within northwestern Ontario.

 doi:10.20944/preprints202312.1133.v1

2.2. Data Acquisition

2.2.1. Validation Data

Validation data was collected by two field crews working independently of one another. Field crews visited each site within three months of one another to ensure site conditions did not change between visits. The first field crew established the VSN plot (e.g., located the plot centers using preassigned GPS coordinates, flagged the plot boundary), then numbered each tree within the plot boundary with a DBH greater than or equal to 7cm in the 11.28m radius VSN plot, and recorded species, status (live versus dead), DBH (recorded to the nearest 0.1cm using a diameter tape) and height. The field crew also measured 1.3m above the point of germination for each tree and painted a line at this height, to ensure subsequent measurements of DBH were recorded at the same height.

The second field crew recorded the species, status, and DBH of all trees larger than 7 cm within a smaller subplot (5m radius) of the VSN plot center. The DBH was recorded to the nearest 0.1cm using a diameter tape. An average of the two DBH values collected by each of the field crews was used as the validation DBH value for each sampled tree. Distance from plot center was recorded to the nearest point on each tree stem at breast height using a clinometer. The distance (m) and azimuth (Degrees) from the plot center to the nearest point on each tree stem to facilitate correlating validation data with trees in the extracted site cross-sections. Azimuth was recorded to the nearest degree using a compass. For each field site, understory was classified into one of five categories of understory density (Minimal: 0-20% of tree stems between 0 and 2.5m are obscured; Low: 21-40% obscured; Moderate: 41-60% obscured, Dense: 61-80% obscured, or Very Dense: 81-100% obscured) based on the amount of leafy vegetation present between 0.5m and 2.5m above the ground when the point clouds were acquired.

2.2.2. LiDAR Data

To prepare sites for LiDAR acquisition, the metal rod at the plot center was flagged with both pink and yellow flagging tape. The 5m radius from plot center to the LiDAR subplot boundary in each of the four cardinal directions was measured using a 30m measuring tape. Tripods were placed at the plot boundary in each of the four cardinal directions to simplify the process of point cloud registration and point matching. The base of all measured, living trees located in each plot were marked with pink flagging tape to facilitate identification of 'in' trees while acquiring LiDAR data. Point clouds were acquired using the Zappcha application and an Apple iPad Pro 12th Generation [10,13]. The circular scanning method that was found to provide the most accurate estimates of DBH was used for point cloud acquisition [11].

2.3. Point Cloud Processing

Point clouds were imported to CloudCompare software from Zappcha app via the Veesus Cloud Plugin for further processing [13,14]. The point clouds were projected and clipped to plot boundaries using ArcGIS Pro [15]. Using the CloudCompare software, point clouds were co-registered for the quadrants in each plot, then cleaned using the 'Statistical Outlier Removal (SOR)' tool [14].

The Cloth Simulation Filtering (CSF) method developed by Zhang et al. (2016) was used to identify points related to the ground in each filtered point cloud and interpolate the ground surface for areas without data [16]. Using the elevation value for the interpolated ground surface, the elevation value representing breast height (1.3 m above ground) for each point cloud was calculated. A single 4 cm tall cross-section centered at breast height was extracted from each non-ground point cloud. Points representing individual features in plot cross-sections were identified and segmented using the density-based clustering algorithm (DBSCAN) in ArcGIS Pro [15]. By cross-referencing the identified clusters with stem maps for each plot, the cluster representing each measured tree was identified. Clusters representing more than one tree were manually split into separate shapefiles. Manual cleaning of the clusters representing measured trees was performed. The X and Y coordinates of each point in the trimmed cluster shapefiles were appended to the attribute tables.

 doi:10.20944/preprints202312.1133.v1

All tree attributes were imported to R, using the 'conicfit' package for curve fitting [17,18]. An iterative geometric ellipse fit was applied to the points in each stem cross-section [11,18]. The iterative ellipse fitting formula used the results of Taubin's Direct-Least Squares Ellipse fitting formula as the initial estimated ellipse parameters for each tree. The iterative ellipse-fitting formula then used the Levenberg-Marquardt method with a maximum of 200 iterations to reduce the error metric of the fitted ellipses [18,19]. Using the geometric parameters for each fitted ellipse, the average diameter of each ellipse was calculated as the estimated DBH (cm).

2.4. Statistical Methods

The average of the DBH values (cm) recorded by the two field crews for each tree were used as the validation DBH values. The difference (cm), absolute error, and relative absolute error between the estimated DBH and the validation DBH were calculated for each tree. The acceptable accuracy level of OMNRF's DBH estimation in forest inventories is 1cm compared to the actual measurements [20]. Hence, this study adapted the same accuracy level.

The absolute error (cm) and relative absolute error (%) of each individual tree were used as measures of accuracy for statistical analyses. Box plots were created for the overall dataset to identify skew and distribution of the results. Kruskal-Wallis tests were used to determine if any of the tested independent variables at the site level (Site type, species class, stand age, stand density, understory class) or individual tree level (tree species, measured DBH size) had statistically significant impacts on the accuracy of estimated DBH values (relative error). For variables with significant impacts on estimate accuracy, a Dunn-Bonferroni post-hoc test was used to determine how different values of that variable impacted estimate accuracy.

3. Results

3.1. Validation Data

The 15 sites varied considerably for live tree density (254 - 2928 stems ha-1), ranged in age from 25-114 years, and had a range of understory densities (Table 1). None of the 15 study sites had all estimated DBH values within 1cm of the measured DBH, ranging from as high as 83.3% (Site MX 81-100) to as low as 0% (Site MX 61-80). The least accurate DBH estimate was a White Spruce (Picea glauca) in plot CON 20-40, with an actual DBH of 12.2cm and an estimated DBH of 7.1cm.

Table 1. Field Site Overview.

Site	Age	Measured Trees *	Density (Stems ha-1) **	Species Composition ***	Average DBH (cm)	Understory Class (1-5)
BRD 20-40	35	19	2419	Pt74 Sb26	13.1	Low (2)
BRD 41-60	45	7	1019	Pt80 Pj10 Bw10	20.9	Dense (4)
BRD 61-80	74	9	1273	By50 Mr50	16.0	Moderate (3)
BRD 81-100	91	8	1146	Pt100	29.7	Moderate (3)
BRD 101+	114	3	764	Pt100	21.5	Very Dense (5)
CON 20-40	27	23	2928	Sb91 Pj9	10.4	Low (2)
CON 41-60	54	12	1528	Bf83 Pt17	19.5	Very Dense (5)
CON 61-80	74	2	382	Pj100	30.6	Low (2)
CON 81-100	91	15	1909	Pj100	21.9	Minimal (1)
CON 101+	105	7	1146	Cw78 Bf11 Bw11	23.8	Minimal (1)
MX 20-40	25	8	1401	Pt64 Pj18 Sb16	17.4	Minimal (1)
MX 41-60	50	8	1146	Bf44 Bw22 Sb22 Ag12	14.9	Moderate (3)
MX 61-80	70	2	254	Sw50 Bw50	28.4	Very Dense (5)
MX 81-100	84	6	764	Pt50 Bf30 Sw20	28.4	Dense (4)
MX 101+	109	4	764	Pj66 Pt34	25.4	Minimal (1)

* Number of measured trees includes only living trees (DBH ≥ 7.0cm) within the 5m sub-plot. ** Density calculated using number of living and dead trees (DBH ≥ 7.0cm) within the 5m sub-plot. *** Species composition

Preprints (www.preprints.org) | NOT PEER-REVIEWED | Posted: 15 December 2023 doi:10.20944/preprints202312.1133.v1

is represented by two-letter species codes: Pt, trembling aspen (*Populus tremuloides)*; Sb, black spruce *(Picea mariana*); Pj, jack pine (*Pinus banksiana*); Bw, white birch (*Betula papyrifera*); By, yellow birch *(Betula alleghaniensis*); Mr, red maple (*Acer rubrum*); Bf, balsam fir (*Abies balsamea*), Cw, eastern white cedar (*Thuja occidentalis*); Ag, green ash (*Fraxinus pennsylvanica*); Sw, white spruce (*Picea glauca*).

Table 3. Comparison between the mean measured and estimated DBH values (cm) and associated MAE (cm and %) for the 15 visited sites.

Site Name	Mean Measured DBH (cm)	Mean Estimated DBH (cm)	MAE (cm)	MAE (%)
BRD 20-40	13.1	12.7	1.1	8.4
BRD 41-60	20.9	20.9	1.3	6.2
BRD 61-80	16.0	15.3	1.6	10.0
BRD 81-100	29.7	29.8	0.6	2.0
BRD 101+	18.7	17.7	1.9	10.2
CON 20-40	10.4	9.4	1.0	9.6
CON 41-60	14.8	14.6	2.0	13.5
CON 61-80	30.6	31.3	0.7	2.3
CON 81-100	21.9	21.9	0.9	4.1
CON 101+	23.8	24.8	1.1	4.6
MX 20-40	17.4	17.3	0.6	3.4
MX 41-60	14.9	13.9	1.2	8.1
MX 61-80	28.4	26.9	1.5	5.3
MX 81-100	26.2	26.1	0.5	1.9
MX 101+	25.4	25.6	1.3	5.1

3.2. Impact of Site- and Tree-Level Factors on Estimation Accuracy

Overall, an RMSE of 1.5cm (8.6%), and an MAE of 1.1cm (6.4%) were achieved in this study. The distribution of the individual tree absolute error values was not normally distributed, and the results skewed towards zero (Figure 2).

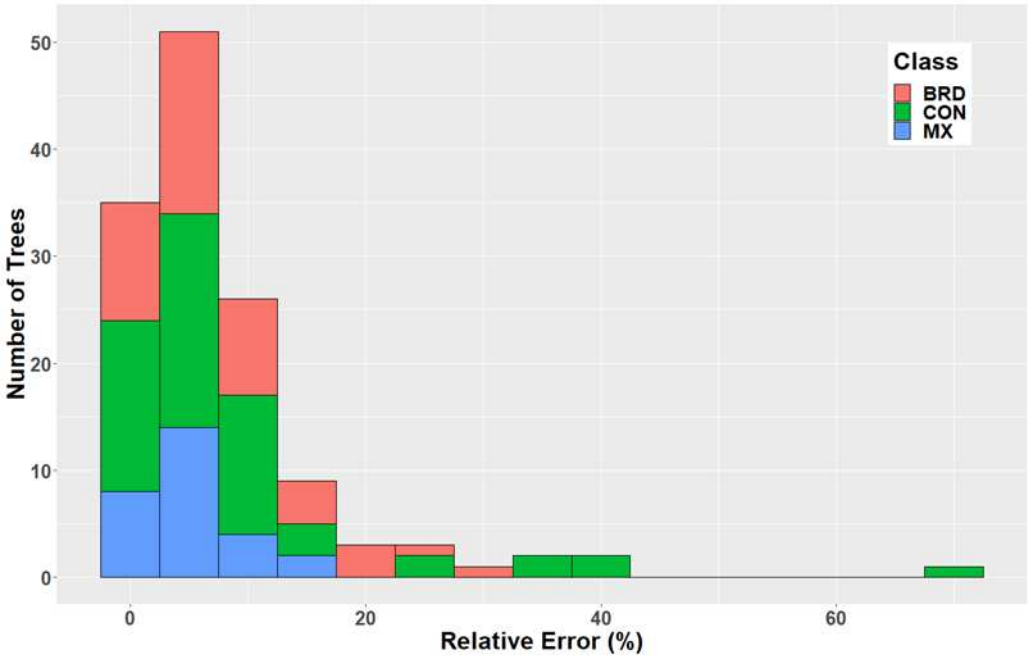

Figure 2. Histogram showing distribution of the number of trees as a function of the relative error values.

Preprints (www.preprints.org) | NOT PEER-REVIEWED | Posted: 15 December 2023 doi:10.20944/preprints202312.1133.v1

The 81-100 age class produced the most accurate estimates of DBH, with an MAE of 0.72cm (3.01%) (Table 4). In terms of stand density effects, the lowest density class (250-500 stems ha-1) produced the most accurate estimates of DBH in terms of relative MAE, with an MAE of 1.13 (3.92%), although this density class only had 4 measured trees. For density classes with 10 or more measured trees, the most accurate estimates of DBH (cm) were achieved in the 501-1000 stems ha-1 density class, which had an MAE of 1.03cm (4.59%; Table 4). The sites with minimal understory produced the most accurate estimates of DBH, with an MAE of 0.91cm (4.06%) (Table 4). Generally, the MAE were comparable across the understory classes 1 (minimal) to 4 (dense), but increased substantially in the very dense class (MAE: 19.4cm and relative MAE of 17.6%). The 25.1-30cm DBH class produced the lowest MAE (0.82cm; 3.02%), while the 30.1-35cm DBH class produced the lowest relative MAE (0.94cm; 2.97%) (Table 4).

Table 4. Number of trees, Mean Absolute Error (cm), and relative Mean Absolute Error (%) as a function of the tested site and species factors.

Factor	Factor Level	Number of Trees	Mean Absolute Error (cm)	Relative Mean Absolute Error (%)
Species Class	Broadleaf	46	1.19	7.30
	Conifer	59	1.16	9.45
	Mixed	28	0.90	4.91
Age Class	20-40	50	0.96	8.19
	41-60	27	1.56	13.05
	61-80	13	1.48	8.94
	81-100	29	0.72	3.01
	101+	14	1.30	5.66
Density Class (Stems ha-1)	250-500	4	1.13	3.92
	500-1000	13	1.03	4.59
	1001-1500	47	1.09	6.24
	1501-2000	12	1.95	19.66
	2001-2500	34	0.98	6.25
	2501-3000	23	1.00	9.88
Understory Class	Minimal (1)	34	0.91	4.06
	Low (2)	44	1.01	8.77
	Moderate (3)	25	1.17	7.34
	Dense (4)	15	0.99	4.87
	Very Dense (5)	15	1.94	17.59
Tree Species	Balsam Fir	17	1.31	14.80
	Black Spruce	35	0.92	8.99
	Cedar	5	0.80	3.39
	Green Ash	1	0.80	7.48
	Jack Pine	13	0.92	3.55
	Red Maple	4	2.02	9.21
	Trembling Aspen	46	1.15	5.72
	White Birch	5	1.26	6.30
	White Spruce	2	1.75	6.31
	Yellow Birch	5	1.32	12.74
DBH Class (cm)	7-10	30	1.08	13.58
	10.1-15	28	1.13	9.49
	15.1-20	23	1.02	5.95
	20.1-25	25	1.32	5.81
	25.1-30	17	0.82	3.02
	30.1-35	5	0.94	2.97
	35.1-40	3	1.13	3.00
	40.1-50	1	4.80	11.46

As highlighted in Figure 2, the data did not follow a normal distribution. The skewness was 3.17 with a Kurtosis value of 16.56, indicating a highly skewed dataset. To determine if any of the above

Preprints (www.preprints.org) | NOT PEER-REVIEWED | Posted: 15 December 2023 doi:10.20944/preprints202312.1133.v1

factors had statistically significant impacts on the accuracy of DBH estimates (relative MAE; %), Kruskal-Wallis tests were therefore used. Age class and density had large magnitudes of effect on the relative accuracy of the estimated DBH values for individual trees (Table 5). Understory classes had a moderate magnitude of effect, while species class had a small effect on the accuracy of estimated DBH values. Age (0.17) and understory classes (0.13) had the greatest effect sizes when examined individually, as well as when examining pairwise interactions (0.23). Species class (0.01) had the smallest effect size on the relative accuracy of estimated DBH values.

Table 5. Kruskal-Wallis test results showing the statistical impact of individual stand- and site-level attributes and significant pairwise interactions on relative accuracy of DBH estimates.

Factor(s)	Df	Test Statistic	*p*-Value	Effect Size	Magnitude Of Effect
Age Class	4	25.95	3.24E-05	0.17	Large
Density Class	5	16.26	6.15E-04	0.09	Moderate
Site Species Class	2	2.78	0.25	0.01	Small
Understory	4	20.40	4.17E-04	0.13	Moderate
DBH Class	8	25.67	1.40E-03	0.14	Moderate
Species	9	12.67	0.18	0.03	Small
Age Class * Density Class	13	39.08	1.94E-04	0.22	Large
Age Class * Site Species Class	14	39.69	2.85E-04	0.22	Large
Age Class * Understory	12	39.34	9.23E-05	0.23	Large
Density Class * Site Species Class	13	37.86	3.04E-04	0.21	Large
Density Class * Understory	14	39.69	2.85E-04	0.22	Large
Site Species Class * Understory	9	25.76	2.23E-03	0.14	Moderate
DBH Class * Age Class	27	43.99	0.02	0.16	Large
DBH Class * Density Class	27	37.83	0.08	0.10	Moderate
DBH Class * Site Species Class	22	39.92	0.01	0.16	Large
DBH Class * Understory	29	55.36	6.43E-03	0.20	Large
Age Class * Species	22	45.91	2.03E-03	0.22	Large
Density Class * Species	22	36.26	0.03	0.13	Moderate
Species * Understory	21	49.49	4.29E-04	0.26	Large

Individual tree species had a small (0.03) effect on relative accuracy of estimated DBH values, whereas DBH size class had a moderate effect (0.14). For the individual site-level attributes that had significant effects on the accuracy of estimated DBH values (age, density, and understory classes), Dunn-Bonferroni post-hoc tests were conducted to identify interactions between two values for a single variable with a significant impact on the accuracy of estimated DBH values (Table 6).

Table 6. Dunn-Bonferroni post-hoc test results showing age classes, DBH categories, density categories, and understory classes with significant statistical differences.

Factor	Group 1	Group 2	N1	N2	Statistic	*p*-Value
Age Class	20-40	81-100	50	29	-3.67	2.39E-04
Age Class	41-60	81-100	27	29	-4.79	1.66E-06
Age Class	61-80	81-100	18	29	-2.92	3.50E-03
DBH Class	7-10cm	25.1-30cm	30	17	-3.71	2.09E-04
DBH Class	10.1-15cm	25.1-30cm	28	17	-3.65	2.61E-04
Density Class	1001-1500	1501-2000	47	12	3.23	1.24E-03
Density Class	1501-2000	2001-2500	12	34	-3.01	2.61E-03
Density Class	1501-2000	501-1000	12	13	-3.4	6.66E-04
Understory	Minimal (1)	Low (2)	34	44	2.85	4.39E-03
Understory	Minimal (1)	Very Dense (5)	34	15	4.08	4.45E-05
Understory	Dense (4)	Very Dense (5)	15	15	3.17	1.50E-03

Preprints (www.preprints.org) | NOT PEER-REVIEWED | Posted: 15 December 2023 doi:10.20944/preprints202312.1133.v1

Below, Figure 3 shows a scatter plot of the estimated DBH (cm) for each individual tree (Colored by site species class), plotted as a function of measured DBH (cm), with a line plotted showing a 1:1 relationship.

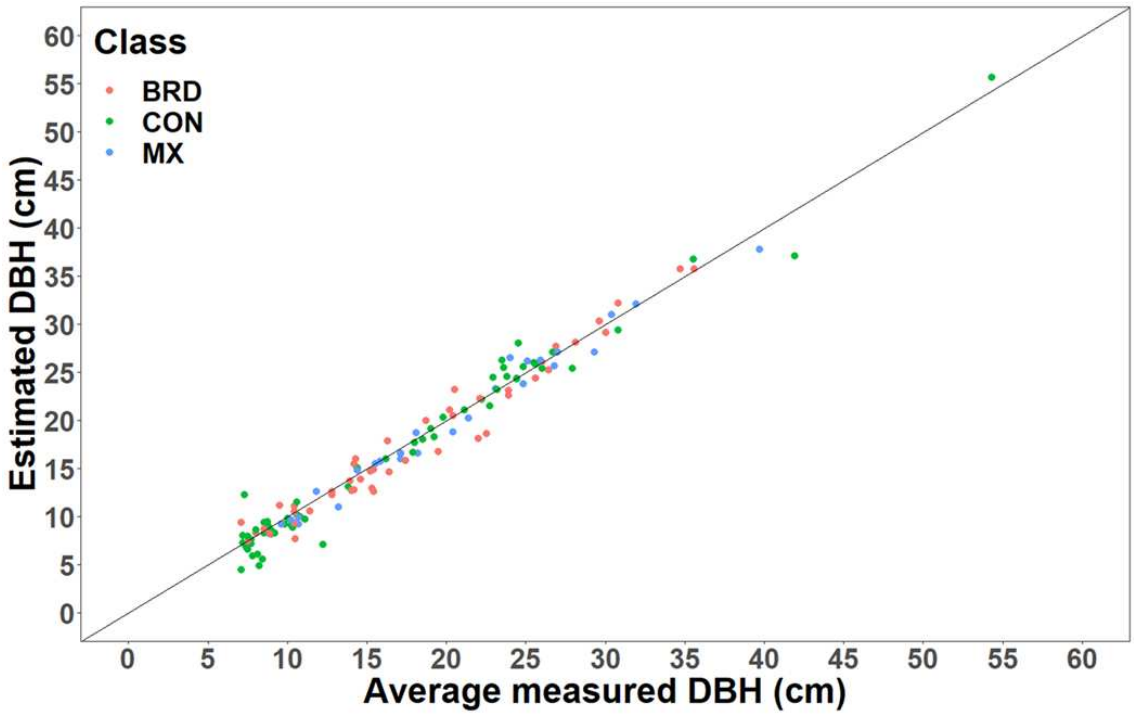

Figure 3. Scatter plot showing estimated DBH (cm) as a function of actual DBH (cm) colored by site species class, with a line modelling a 1:1 relationship.

74 trees had estimated DBH values lower than the actual DBH values (55.6% of measured trees), with 53 estimated DBH values greater than the actual DBH values (39.9% of measured trees), with an additional 6 trees (4.5% of measured trees) having an estimated DBH equal to the actual DBH.

The pairwise interaction with the largest effect size was between individual tree species and understory classes (Table 5). Interactions between individual tree DBH size class and age class, species class, and understory class all had large effects (> 0.10) on the relative accuracy of individual tree DBH estimates. Overall, age class, individual tree DBH size class, and site understory classes had the largest effects on the accuracy of individual tree DBH estimates (Table 5).

4. Discussion

This study achieved an overall RMSE of 1.5cm (8.6%) for DBH values estimated from iPad Pro LiDAR data for 15 sites in the boreal forest. This is a lower RMSE than those reported in several previous studies using the iPad Pro to estimate DBH, such as: an urban park (Slovakia), 2.8cm (7.0%) and 5.2cm (13.0%); a research forest (Austria), 3.1cm (10.5%) and 6.3cm (21.2%); Natural and plantation forests (Japan), 2.3cm (10.5%); and, a university campus (Türkiye), 2.3cm (11.7%) [5,21–23]. A previous study using the same methodology as used in this study reported an RMSE of 1.1cm (6.2%) for a plantation forest in Canada [11].

This study set out to investigate the effects of various site-level (Age Class, Species Class, Tree Density, Understory Density) and tree-level (Tree Species, Actual DBH) attributes on the relative accuracy of DBH values estimated using point cloud data acquired by an iPad Pro LiDAR scanner. It was found that all tested variables, with the exception of species class and individual tree species, had moderate to large magnitudes of effect on the relative accuracy of estimated DBH values (Tables 10–13). The secondary objective was to identify specific site conditions that facilitate or inhibit accurate estimation of DBH using the iPad Pro LiDAR scanner. While some trends were identified in the data, the results do not conclusively identify specific site conditions that facilitate or inhibit

accurate estimation of DBH. Generally, sites with lower tree densities and less understory vegetation improved accuracy of DBH estimates, as did the measurement of larger trees (Table 4). In contrast, individual tree species, species composition, and stand age were not found to significantly affect the relative accuracy of estimated DBH values (Table 5).

It was hypothesized that DBH estimate accuracy would be lower in stands with significant leafy tissue or other obstructions at or around breast height (i.e., stands with high understory plant cover or stands with high tree densities). Our results showed that DBH estimates were most accurate in stands with minimal understory (Table 4). However, the results also show the understory class with the second most accurate estimates of DBH was the second-densest understory class. Understory class did have a moderate magnitude of effect on the relative accuracy of DBH estimates (Table 5). However, Dunn-Bonferroni post-hoc test for differences between levels of understory density suggested differences in the accuracies of estimated DBH values between these groups did not follow any trends (Table 6).

It was also hypothesized that the most accurate estimates of DBH would be achieved on sites with lower tree densities. Our results found that the lower three density classes (250-500 stems ha-1; 501-1000 stems ha-1; 1001-1500 stems ha-1) had more accurate estimates of DBH (Table 4). However, significant differences were observed between the 501-1000 and 1501-2000 stems ha-1 density classes; the 1001-1500 and 1501-2000 stems ha-1 classes; and, the 1501-2000 and 2001-2500 stems ha-1 classes. The most extreme density classes, 250-500 stems ha-1 and 2501-3000 stems ha-1, were not significantly different from one another or any of the other tested density classes. The lack of significant differences in estimate accuracy between the lowest and highest site density classes and the rest of the dataset suggests that site density alone is not sufficient to predict the accuracy of DBH estimates.

The final hypothesis suggested that the relative error of DBH estimates would decrease as tree size increased. With the exception of the sole tree in the 40cm+ DBH class, relative error of DBH estimates decreased as tree size increased. Discarding the three size classes with 5 or fewer measured trees (30.1-35cm; 35.1-40cm; 40.1-50cm), the 25.1-30cm DBH class was the size class with the largest measured DBH values, and had the lowest relative error (Table 4). Dunn-Bonferroni post-hoc testing found significant differences between the 25.1-30cm DBH class and both the 7-10cm and 10.1-15cm DBH classes (Table 6). This demonstrates that increases in actual DBH reduced the relative error of estimated DBH values in a statistically significant manner.

Understory density was not considered when selecting sites for this study, as only site species composition and site age were known during the site selection period. As a result, the different combinations of understory density, site species class, and site age class were not evenly distributed, potentially causing bias in the results for the impact of understory density on the relative accuracy of estimated DBH values. Future research should incorporate multiple replicates of each combination of site species/age class to capture as much variation in understory density for that species/age class combination as possible.

Common causes of error identified in previous studies using the iPad Pro include IMU errors with the iPad Pro, as well as high proportions of misplaced points ('noise') in acquired point clouds [5,21]. IMU errors contribute to scanned features with low surface fidelities, especially when significant movement occurs during the acquisition of a given point cloud [24,25]. Other factors contributing to IMU errors include changes in walking speed, rapid movements, or turning the iPad during the course of a scan [5,11,21,23]. IMU errors were present in this study as well, with misaligned tree cross-sections encountered several times. The misalignments were manually corrected, although this introduced a potential cause of error. High levels of error in point location (-/+1cm) in point clouds acquired with the iPad Pro LiDAR scanner have been found to cause trees to appear 'fuzzy' in the point clouds, which caused increased levels of error as tree size decreased [5]. This was also found in this study, with the relative accuracy of estimated DBH values lowest in the smallest DBH class and relative accuracy improving as actual DBH increased (Table 4).

Comparing the results of this study to previous studies using MLS or TLS in natural forests, RMSE values of 2.7cm (10.8%; RANSAC method), 4.1cm (16.3%; Circle Fit), and 6.8cm (27.0%; Voxelization) were found in a study in a black pine (*Pinus nigra*) plantation forest in Italy [2]. It was

 doi:10.20944/preprints202312.1133.v1

found that the accuracy of estimated DBH values was consistent for all sizes of tree recorded in the study. An MAE of 4.8cm (25.9% RMSE) was achieved using MLS and an MAE of 5.0cm (27.9% RMSE) using TLS to estimate DBH in a Ponderosa pine (*Pinus ponderosa*) forest in northern Arizona [8]. An RMSE of 2.4cm (5.6%) was achieved using TLS in managed Japanese cedar (*Cryptomeria japonica*) forests in Japan [9]. Common causes of inaccuracy include occlusion of scanned trees from understory vegetation [8,9].

The results presented here support previous studies that found IMU errors, positional accuracy errors, and high levels of noise in point clouds to cause reduced accuracy of DBH values estimated using the iPad Pro LiDAR scanner. Factors identified as contributing to inaccuracies in previous studies using MLS or TLS to estimate DBH, such as high levels of understory vegetation or high site densities, were also found to reduce the accuracy of estimated DBH values with the iPad Pro. While tree size was found to impact the accuracy of DBH estimates both here and in previous studies using the iPad Pro LiDAR scanner, this factor did not impact the accuracy of DBH values estimated from TLS or MLS devices in previous studies, suggesting that this limiting factor is unique to the iPad Pro.

5. Conclusions

Although there were no tested sites where all estimated DBH values fell within the acceptable margin of error (1cm based on OMNRF standards), this methodology estimated DBH values for all 133 scanned trees, with 78 of the estimated DBH values (59%) falling within the acceptable margin of error and 11 estimated DBH values (7%) within 0.1cm of the validation value. It was found that site and understory density had statistically significant impacts on the accuracy of estimated DBH values, while site species class did not (Table 5). At the individual tree level, the actual DBH of a tree had a moderate effect on the accuracy of estimated DBH values, while individual tree species did not (Table 5).

Trends in the data suggested that increased density of both trees and understory vegetation on a given site would decrease the accuracy of estimated DBH values on the site, as hypothesized. Examining differences between the understory and site density classes with Dunn-Bonferroni post-hoc testing, it was found that these factors had significant impacts on the relative accuracy of estimated DBH values. However, the differences between different classes of these variables did not present a consistent or continuous relationship, with no strong trends present. Increases in actual tree size led to increases in the relative accuracy of estimated DBH values. Dunn-Bonferroni post-hoc testing showed that the relative accuracy of estimated DBH values improved as measured tree size increased, supporting this hypothesis.

The results of this study suggest that the significant impacts of site understory, actual tree size, age class, and density will impact the accuracy of estimated DBH values in future studies using the iPad Pro to estimate DBH, and must be addressed and characterized in future studies to better contextualize results in a broader context. At this point in time, the persistent issues with the iPad Pro IMU and positional accuracy errors limit accuracy of DBH estimates attainable with the iPad Pro LiDAR scanner in natural boreal forests. Additionally, the use of iPad Pro LiDAR for forest inventory is limited by an inability to perform well in unfavorable weather conditions, such as rain, fog, or wind, limiting the operational feasibility of this method at the industry scale. The iPad Pro shows promise, meeting accuracy specifications for 59% of the scanned trees across 15 sites representing a range of site conditions in boreal forests. However, current limitations prevent this device from being operationalizable in the boreal forest to replace manual mensuration of DBH for forest inventories.

Author Contributions: Conceptualization, M.G., M.K.H., D.M and BL.; methodology, M.G., M.K.H., D.M and B.L; formal analysis, M.G..; writing—original draft preparation, M.G.; writing—review and editing, M.K.H., D.M and BL.; supervision, M.K.H., D.M and BL. All authors have read and agreed to the published version of the manuscript.

Funding: This project was partially funded by a "Graduate Assistantship" with the Faculty of Natural Resources Management at Lakehead University. Fieldwork was supported by the Forest Resource Inventory Unit and the Center for Northern Forest Ecosystem Research, both of the Ontario Ministry of Natural Resources and Forestry.

Data Availability Statement: The data presented in this study is available on request from the corresponding author.

Acknowledgments: Thanks to Geordie Robere-McGugan of the Ontario Forest Resource Inventory Unit for helping setup 2023 fieldwork; Kyle Webb, Domenic McVey, and Josh Oleksuk of the Center for Northern Forest Ecosystem Research for their assistance conducting fieldwork.

Conflicts of Interest: The authors declare no conflict of interest.

References

1. Bauwens, S.; Bartholomeus, H.; Calders, K.; Lejeune, P. Forest Inventory with Terrestrial LiDAR: A Comparison of Static and Hand-Held Mobile Laser Scanning. *Forests* **2016**, *7*, 127, doi:10.3390/f7060127.
2. Chiappini, S.; Pierdicca, R.; Malandra, F.; Tonelli, E.; Malinverni, E.S.; Urbinati, C.; Vitali, A. Comparing Mobile Laser Scanner and Manual Measurements for Dendrometric Variables Estimation in a Black Pine (Pinus Nigra Arn.) Plantation. *Computers and Electronics in Agriculture* **2022**, *198*, 107069, doi:10.1016/j.compag.2022.107069.
3. Aijazi, A.K.; Checchin, P.; Malaterre, L.; Trassoudaine, L. Automatic Detection and Parameter Estimation of Trees for Forest Inventory Applications Using 3D Terrestrial LiDAR. *Remote Sensing* **2017**, *9*, 946, doi:10.3390/rs9090946.
4. Balenović, I.; Liang, X.; Jurjević, L.; Hyyppä, J.; Seletković, A.; Kukko, A. Hand-Held Personal Laser Scanning: Current Status and Perspectives for Forest Inventory Application. *Croat. j. for. eng. (Online)* **2021**, *42*, 165–183, doi:10.5552/crojfe.2021.858.
5. Gollob, C.; Ritter, T.; Kraßnitzer, R.; Tockner, A.; Nothdurft, A. Measurement of Forest Inventory Parameters with Apple iPad Pro and Integrated LiDAR Technology. *Remote Sensing* **2021**, *13*, 3129, doi:10.3390/rs13163129.
6. Hunčaga, M.; Chudá, J.; Tomaštík, J.; Slámová, M.; Koreň, M.; Chudý, F. The Comparison of Stem Curve Accuracy Determined from Point Clouds Acquired by Different Terrestrial Remote Sensing Methods. *Remote Sensing* **2020**, *12*, 2739, doi:10.3390/rs12172739.
7. Wang, F.; Heenkenda, M.K.; Freeburn, J.T. Estimating Tree Diameter at Breast Height (DBH) Using an iPad Pro LiDAR Sensor. *Remote Sensing Letters* **2022**, *13*, 568–578, doi:10.1080/2150704X.2022.2051635.
8. Donager, J.J.; Sánchez Meador, A.J.; Blackburn, R.C. Adjudicating Perspectives on Forest Structure: How Do Airborne, Terrestrial, and Mobile Lidar-Derived Estimates Compare? *Remote Sensing* **2021**, *13*, 2297, doi:10.3390/rs13122297.
9. Shimizu, K.; Nishizono, T.; Kitahara, F.; Fukumoto, K.; Saito, H. Integrating Terrestrial Laser Scanning and Unmanned Aerial Vehicle Photogrammetry to Estimate Individual Tree Attributes in Managed Coniferous Forests in Japan. *International Journal of Applied Earth Observation and Geoinformation* **2022**, *106*, 102658, doi:10.1016/j.jag.2021.102658.
10. Apple Apple Unveils New iPad Pro with LiDAR Scanner and Trackpad Support in iPadOS Available online: https://www.apple.com/newsroom/2020/03/apple-unveils-new-ipad-pro-with-lidar-scanner-and-trackpad-support-in-ipados/ (accessed on 6 December 2022).
11. Guenther, M.; Heenkenda, M.K.; Leblon, B.; Morris, D.; Freeburn, J.T. Estimating Tree Diameter at Breast Height (DBH) Using iPad Pro Light Detection and Ranging (LiDAR) Sensor in Boreal Forests. *Canadian Journal of Remote Sensing* **2023**. *Accepted*
12. Morris, D. Personal Communication 2023.
13. Veesus ZAPPCHA: Mobile LiDAR Scanner 2022.
14. Girardeau-Montaut, D. CloudCompare - Open Source Project 2022.
15. ESRI ArcGIS Pro 2023.
16. Zhang, W.; Qi, J.; Wan, P.; Wang, H.; Xie, D.; Wang, X.; Yan, G. An Easy-to-Use Airborne LiDAR Data Filtering Method Based on Cloth Simulation. *Remote Sensing* **2016**, *8*, 501, doi:10.3390/rs8060501.
17. Bivand, R.; Keitt, T.; Rowlingson, B.; Pebesma, E.; Sumner, M.; Hijmans, R.; Baston, D.; Rouault, E.; Warmerdam, F.; Ooms, J.; et al. Rgdal: Bindings for the "Geospatial" Data Abstraction Library 2023.
18. Chernov, N.; Gama, J. Conicfit: Algorithms for Fitting Circles, Ellipses and Conics 2015.
19. Taubin, G. Estimation of Planar Curves, Surfaces, and Nonplanar Space Curves Defined by Implicit Equations with Applications to Edge and Range Image Segmentation. *IEEE Transactions on Pattern Analysis and Machine Intelligence* **1991**, *13*, 1115–1138, doi:10.1109/34.103273.

20. Ontario Ministry of Natural Resources and Forestry *Vegetation Sampling Network Protocol: Technical Specifications for Field Plots.*; 2.0.; Ontario Ministry of Natural Resources and Forestry, Science and Research Branch: Peterborough, ON, 2021;
21. Wang, X.; Singh, A.; Pervysheva, Y.; Lamatungga, K.E.; Murtinová, V.; Mukarram, M.; Zhu, Q.; Song, K.; Surový, P.; Mokroš, M. Evaluation of iPad Pro 2020 LiDAR for Estimating Tree Diameters in Urban Forest. *ISPRS Ann. Photogramm. Remote Sens. Spatial Inf. Sci.* **2021**, *VIII-4/W1-2021*, 105–110, doi:10.5194/isprs-annals-VIII-4-W1-2021-105-2021.
22. Tatsumi, S.; Yamaguchi, K.; Furuya, N. ForestScanner: A Mobile Application for Measuring and Mapping Trees with LiDAR-Equipped iPhone and iPad. *Methods in Ecology and Evolution* **2021**, *0*, *7*, doi:10.1111/2041-210X.13900.
23. Gülci, S.; Yurtseven, H.; Akay, A.O.; Akgul, M. Measuring Tree Diameter Using a LiDAR-Equipped Smartphone: A Comparison of Smartphone- and Caliper-Based DBH. *Environ Monit Assess* **2023**, *195*, 678, doi:10.1007/s10661-023-11366-8.
24. Tavani, S.; Billi, A.; Corradetti, A.; Mercuri, M.; Bosman, A.; Cuffaro, M.; Seers, T.; Carminati, E. Smartphone Assisted Fieldwork: Towards the Digital Transition of Geoscience Fieldwork Using LiDAR-Equipped iPhones. *Earth-Science Reviews* **2022**, *227*, 103969, doi:10.1016/j.earscirev.2022.103969.
25. Corradetti, A.; Seers, T.; Mercuri, M.; Calligaris, C.; Busetti, A.; Zini, L. Benchmarking Different SfM-MVS Photogrammetric and iOS LiDAR Acquisition Methods for the Digital Preservation of a Short-Lived Excavation: A Case Study from an Area of Sinkhole Related Subsidence. *Remote Sensing* **2022**, *14*, 5187, doi:10.3390/rs14205187.